

Magnetoelectric write and read operations in a stress-mediated multiferroic memory cell

Alexey Klimov, Nicolas Tiercelin, Yannick Dusch, Stefano Giordano, Théo Mathurin, Philippe Pernod, Vladimir Preobrazhensky, Anton Churbanov, and Sergei Nikitov

Citation: *Appl. Phys. Lett.* **110**, 222401 (2017); doi: 10.1063/1.4983717

View online: <http://dx.doi.org/10.1063/1.4983717>

View Table of Contents: <http://aip.scitation.org/toc/apl/110/22>

Published by the [American Institute of Physics](#)



**FIND THE NEEDLE IN THE
HIRING HAYSTACK**

POST JOBS AND REACH THOUSANDS OF
QUALIFIED SCIENTISTS EACH MONTH.

PHYSICS TODAY | JOBS
WWW.PHYSICSTODAY.ORG/JOBS

Magnetoelectric write and read operations in a stress-mediated multiferroic memory cell

Alexey Klimov,^{1,2,3} Nicolas Tiercelin,² Yannick Dusch,² Stefano Giordano,² Théo Mathurin,² Philippe Pernod,² Vladimir Preobrazhensky,^{2,4} Anton Churbanov,^{1,5} and Sergei Nikitov^{1,5}

¹Joint International Laboratory LIA LICs: V. A. Kotel'nikov Institute of Radioeng. and Electronics (IRE RAS), ul. Mokhovaya 11/7, Moscow 125009, Russia

²Joint International Laboratory LIA LICs: University Lille, CNRS, Centrale Lille, ISEN, University Valenciennes, UMR 8520 - IEMN, F-59000 Lille, France

³Joint International Laboratory LIA LICs: Moscow Technological University (MIREA) Vernadsky Avenue 78, Moscow 119454, Russia

⁴Joint International Laboratory LIA LICs: Wave Research Center, A.M.Prokhorov GPI, RAS, ul. Vavilova 38, Moscow 119991, Russia

⁵Moscow Institute of Physics and Technology, Dolgoprudny, Institutskiy lane, 9, 141700, Russia

(Received 20 February 2017; accepted 4 May 2017; published online 30 May 2017)

Magnetic memory cells associated with the stress-mediated magnetoelectric effect promise extremely low bit-writing energies. Most investigations have focused on the process of writing information in memory cells, and very few on readout schemes. The usual assumption is that the readout will be achieved using magnetoresistive structures such as Giant Magneto-Resistive stacks or Magnetic Tunnel Junctions. Since the writing energy is very low in the magnetoelectric systems, the readout energy using magnetoresistive approaches becomes non negligible. Incidentally, the magneto-electric interaction itself contains the potentiality of the readout of the information encoded in the magnetic subsystem. In this letter, the principle of magnetoelectric readout of the information by an electric field in a composite multiferroic heterostructure is considered theoretically and demonstrated experimentally using $[N \times (\text{TbCo}_2/\text{FeCo})]/[\text{Pb}(\text{Mg}_{1/3}\text{Nb}_{2/3})\text{O}_3]_{(1-x)} - [\text{PbTiO}_3]_x$ stress-mediated ME heterostructures. *Published by AIP Publishing.* [<http://dx.doi.org/10.1063/1.4983717>]

The new generation of data storage technology requires high speed, high density, low power, and nonvolatile random access memory (RAM).^{1,2} Prospective RAMs using different physical principles (Ferroelectric-RAM, Magnetic-RAM, Spin Torque Transfer-RAM, Resistive-RAM, Conductive Bridge RAM, and Phase Change RAM) have been widely discussed in the last few years,³ and for a decade, magnetic RAMs have been foreseen as the strongest contender, especially with the advent of Spin Transfer Torque (STT) and Spin Orbit Torque (SOT)-RAMs.^{4,5} However, these two technologies require large current densities to switch the magnetization between memory states and are therefore far from being optimum.⁶ For this reason, the control of magnetization with electric fields is of prime interest,^{7,8} and a number of works were related on multiferroics and magnetoelectric (ME) effects and compounds for memory applications.^{9–12}

Among the different solutions to achieve the ME effect, it has been shown that coupling the magnetoelastic and piezoelectric materials through mechanical interaction¹³ could yield very energy-efficient memory devices^{14–19} with simulated energy consumptions as low as a few tens of attojoules per written bit.^{20–23} Because of the symmetry of the Joule magnetostriction, which is the main phenomenon at play, many proposed devices rely on the anisotropic nature of the piezo-strain generated by the electric field, and $[\text{Pb}(\text{Mg}_{1/3}\text{Nb}_{2/3})\text{O}_3]_{(1-x)} - [\text{PbTiO}_3]_x$ (PMN-PT) compounds in the $\langle 011 \rangle$ cut are often chosen as an electroactive substrate.^{24,25} Another approach uses nonspecific piezoelectric materials in which an anisotropic stress distribution can be tailored using planar electrodes.^{14,22,26,27} In any of those

configurations of stress-mediated magnetoelectric memory, most investigations have focused on the process of writing information in the memory cell, and very few on the readout schemes. The usual assumption is that the readout will be achieved using magnetoresistive structures such as Giant Magneto-Resistive (GMR) stacks²⁸ or Magnetic Tunnel Junctions (MTJ).²⁷ Although they have been experimentally demonstrated, the integration of these complex elements at a very low scale together with “exotic” electro-active substrates such as PMN-PT and the control micro-electronics remains a challenge. It is also worth noting that, since the writing energy is potentially very low in the ME systems, the readout energy using magnetoresistive approaches becomes non negligible.²⁹ In this respect, alternative readout ways are of high interest.

Incidentally, the ME interaction itself contains the potentiality of the readout of the information encoded in the magnetic subsystem. Because the system is fully coupled, the reorientation of magnetic moments by electric field induces an elastic stress in the piezoelectric layer and generates a piezoelectric potential in the structure. This ME potential depends on the initial state of the magnetic subsystem. If the magnetic state is not modified by the applied electric field, no ME voltage is induced on the piezoelectric layer. On the other hand, if the polarity of the applied electric field corresponds to the reorientation of the magnetic moments, a ME potential should appear. Like the ME writing, the advantage of a ME readout is that it is performed through an electric field and therefore does not require any current going through highly resistive tunnel junctions. Because it relies on the same physical principle, the ME readout requires an

energy as low as the ME writing. In previous theoretical studies, we have demonstrated that the required energy for writing a bit in a 50 nm stress-mediated memory cell is in the 2×10^{-16} J/bit range, which is mainly due to the dissipated energy during the charge/discharge of the capacitor formed by the $\text{Pb}(\text{Zr}_x\text{Ti}_{1-x})\text{O}_3$ (PZT) piezoelectric material between the driving electrodes.²³ For PMN-PT with four times higher piezoelectric constants the expected energy consumption is one order of value smaller. As a comparison, a typical 45 nm Spin Torque Transfer Magnetic memory (STT-RAM) based on a Magnetic Tunnel Junction (MTJ) with a resistance-area product of $10 \Omega \mu\text{m}^2$ leads to a MTJ resistance of $5 \text{ k}\Omega$. For sense currents in the lowest end of the required values, that is to say, $10 \mu\text{A}$, and an optimistic readout time of 1 ns (those values are usually higher for an accurate readout of the stored information), the reading energy lost in Joule heating will still be of 5×10^{-16} J/bit^{30,31} which is more or at best comparable with what could be achieved using the ME readout. In the present paper, we theoretically describe and experimentally demonstrate the principle of both writing and reading information using an electric field in $[N \times (\text{TbCo}_2/\text{FeCo})]/\text{PMN-PT}$ stress-mediated ME heterostructures.

The MagnetoElectric Random Access Memory (MELRAM)^{14,15,25,32} cell shown schematically in Fig. 1 consists of a uniaxial magnetostrictive multilayered structure with N layers of $\text{TbCo}_2/\text{FeCo}$ deposited on a PMN-PT piezoelectric crystal in the $\langle 011 \rangle$ cut.²⁵ A magnetic field with a strength H is applied in the plane of the structure normally to the anisotropy axis EA directed at an angle $\pi/4$ with respect to the x axis. If the value of H is smaller than the anisotropy field H_A , the equilibrium state of the magnetic subsystem is bistable. This bistability results from the symmetry of the thermodynamic potential F_m of the magnetic subsystem

$$F_m = -MH \cos \varphi - \frac{1}{2}MH_A \sin^2 \varphi, \quad (1)$$

where M is the value of the saturation magnetization and φ is the angle between the magnetic field and magnetization direction in the plane of the structure. When $H = H_A/\sqrt{2}$, the potential energy F_m has two minima corresponding to the angles of magnetization $\varphi = \pm\pi/4$. These two equilibrium

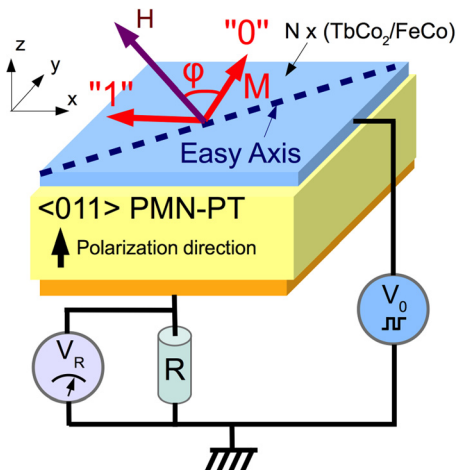


FIG. 1. MELRAM cell and the electric scheme for the magnetic state identification.

states are associated with the bit states “0” and “1”. The switch between these states, corresponding to the information recording, is achievable by an anisotropic in-plane stress within the film associated with the magnetoelastic interaction and described by the energy density

$$F_{me} = -\frac{B}{2(C_{11}^m - C_{12}^m)} (T_{xx}^m - T_{yy}^m) \sin 2\varphi, \quad (2)$$

where the index m indicates the magnetic film, T_{ij}^m is the stress tensor in the magnetic film, C_{ij}^m are its elastic moduli, and B is the magnetoelastic constant. An applied anisotropic stress breaks the symmetry of the thermodynamic potential and results in only one equilibrium state for the magnetization depending on the sign of the stress. If the magnetic system was already in the corresponding state prior to the application of the stress, it will remain unchanged. In the opposite case, the system will switch to the new state upon application of the stress and remain stable in the said state after the stress is released. The dynamics of the magnetic switch in the system under consideration have already been described in detail.^{14,20,21,23} The energy efficient way for the creation of the stress in a magnetic film is the application of an electric field to the piezoelectric crystal that is elastically coupled to the film. For this purpose, and as it follows from Eq. (2), the in-plane stress should be anisotropic. From a memory cell design point of view, the most appropriate orientation of the electric field \vec{E} is normal to the plane of the structure. This requirement is satisfied, for example, by using a PMN-PT ferroelectric relaxor in the $\langle 011 \rangle$ cut. The correspondent piezoelectric energy density for such a crystal is

$$F_p = -(d_{31}T_{xx}^p + d_{32}T_{yy}^p)E, \quad (3)$$

where d_{ij} is the piezoelectric tensor and T_{ij}^p is the stress tensor in the piezoelectric material. The piezoelectric polarization that is detectable by electrical means is equal to

$$P = -\frac{\partial F_p}{\partial E} = d_{31}T_{xx}^p + d_{32}T_{yy}^p. \quad (4)$$

The quasistatic in-plane deformations, which are the same for both magnetic and piezoelectric layers, can be found using Eqs. (2) and (3) as follows:

$$\begin{aligned} u_{xx} &= S_{11}^m T_{xx}^m + S_{12}^m T_{yy}^m + \frac{B}{2(C_{11}^m - C_{12}^m)} \sin 2\varphi \\ &= S_{11}^p T_{xx}^p + S_{12}^p T_{yy}^p + d_{31}E, \end{aligned} \quad (5)$$

$$\begin{aligned} u_{yy} &= S_{21}^m T_{xx}^m + S_{22}^m T_{yy}^m + \frac{B}{2(C_{11}^m - C_{12}^m)} \sin 2\varphi \\ &= S_{21}^p T_{xx}^p + S_{22}^p T_{yy}^p + d_{32}E, \end{aligned} \quad (6)$$

where S_{ij}^m and S_{ij}^p are the elastic compliance tensors for the magnetic and piezoelectric materials, respectively. The quasi-static conditions of a mechanically free structure are

$$\begin{aligned} h^p T_{xx}^p + h^m T_{xx}^m &= 0, \\ h^p T_{yy}^p + h^m T_{yy}^m &= 0, \end{aligned} \quad (7)$$

where h^m and h^p are the thicknesses of magnetic and piezoelectric layers, respectively. The solutions of Eqs. (6) and (7) are

$$T_{xx}^p = \frac{1}{S_1 S_2 - S_6^2} \left[\begin{array}{l} (d_{32} S_6 - d_{31} S_2) E \\ + (S_2 + S_6) \frac{B}{2(C_{11}^m - C_{12}^m)} \sin 2\varphi \end{array} \right], \quad (8)$$

$$T_{yy}^p = \frac{1}{S_1 S_2 - S_6^2} \left[\begin{array}{l} (d_{31} S_6 - d_{32} S_1) E \\ + (S_1 + S_6) \frac{B}{2(C_{11}^m - C_{12}^m)} \sin 2\varphi \end{array} \right],$$

where the effective compliance parameters are $S_1 = S_{11}^p + \frac{h^p}{h^m} S_{11}^m$, $S_2 = S_{22}^p + \frac{h^p}{h^m} S_{22}^m$ and $S_6 = S_{12}^p + \frac{h^p}{h^m} S_{11}^m$. Taking into account Eq. (7), it follows that Eq. (8) defines the magneto-electric (ME) stress as

$$(T_{xx}^m - T_{yy}^m)_{ME} = \frac{h^p}{h^m} \left[\begin{array}{l} d_{32}(S_1 + S_6) \\ -d_{31}(S_2 + S_6) \end{array} \right] \frac{E}{S_1 S_2 - S_6^2}. \quad (9)$$

This stress contributes to the magnetoelastic energy in Eq. (2) and induces the switch of the magnetization vector through the electric field applied to the piezo-layer. On the other hand, the magnetostrictive part of the stress in Eq. (8) is responsible for the ME polarization

$$P_{ME} = \frac{B}{2(C_{11}^m - C_{12}^m)} \sin 2\varphi \frac{[d_{31}(S_2 + S_6) - d_{32}(S_1 + S_6)]}{S_1 S_2 - S_6^2}. \quad (10)$$

In the typical experimental conditions where $\frac{h^p}{h^m} \ll 1$ the compliance parameters fulfill $S_1 = S_2$ and $S_{11}^m - S_{12}^m = (C_{11}^m - C_{12}^m)^{-1}$. Hence, the expressions of the ME energy density F_{ME} and the polarization P_{ME} are

$$F_{ME} = \frac{1}{2} B (d_{31} - d_{32}) E \sin 2\varphi \quad (11)$$

and

$$P_{ME} = \frac{h^m}{2h^p} B (d_{31} - d_{32}) \sin 2\varphi. \quad (12)$$

Equation (12) describes the magnetic feedback on the electric polarization that allows for the detection of the switch between different magnetic states defined by the magnetization directions. In the simplest electrical scheme shown in Fig. 1, the magnetic switch contributes to the output voltage V_R

$$V_R = V_0 e^{-t/\tau} + \frac{h^p}{\varepsilon_0 \varepsilon_{33}} \int_0^t dt' e^{-(t-t')/\tau} \frac{\partial P_{ME}}{\partial t'}, \quad (13)$$

where $\tau = RC$ with C being the cell capacity and ε_{33} is the z component of the dielectric permittivity of the piezoelectric material. For switching times much smaller than τ , the magneto-electric signal V_{ME} , described by the second term in Eq. (13), is proportional to the variation of polarization ΔP_{ME} during the reorientation of the magnetization between the positions $\varphi = \pm\pi/4$

$$V_{ME} = \frac{h^p}{\varepsilon_0 \varepsilon_{33}} \Delta P_{ME} e^{-t/\tau} = \pm (d_{31} - d_{32}) B \frac{h^m}{\varepsilon_0 \varepsilon_{33}} e^{-t/\tau}. \quad (14)$$

Consequently, this ME signal indicates the magnetization switch induced by the electric field and reveals the

initial state of the magnetic subsystem. For example, if the applied voltage V_0 is positive, the switch is possible only if the initial state corresponds to “0”. If it corresponds to “1” no switch and therefore no ME signal are expected. On the other hand, for a negative voltage the signal can be measured if the initial state is “1.” Thus, the magneto-electric interaction is applicable not only for recording a bit but also for reading the information *via* an electric field in the MELRAM cell.

The experiments were carried out on a cell consisting of a nanostructured magnetostrictive film of 25 bilayers $(\text{TbCo}_2)_{4nm}/(\text{FeCo})_{4nm}$ deposited by RF sputtering on a $10 \times 10 \times 0.3 \text{ mm}^3$ commercial PMN-PT (011) crystalline substrate. The measurements were made using the electrical scheme shown in Fig. 1. The results are presented in Fig. 2. Figure 2(a) shows the sequence of electric pulses $V_0(t)$ applied to the scheme. After each pulse, the cell capacity is discharged. Fig. 2(b) displays the V_R voltage pulses that are detected across the resistance R . Figure 2(c) shows the ME signal $V_{ME} = V_R(H) - V_R(0)$ obtained by subtraction of the signals measured when the magnetizing field was equal to $H = H_A/\sqrt{2}$ and $H=0$. In the last case, where $H=0$, no switch of magnetization is possible independently of the sign of the applied electric voltage. The application of the primary “writing” electric pulse results in the orientation of the

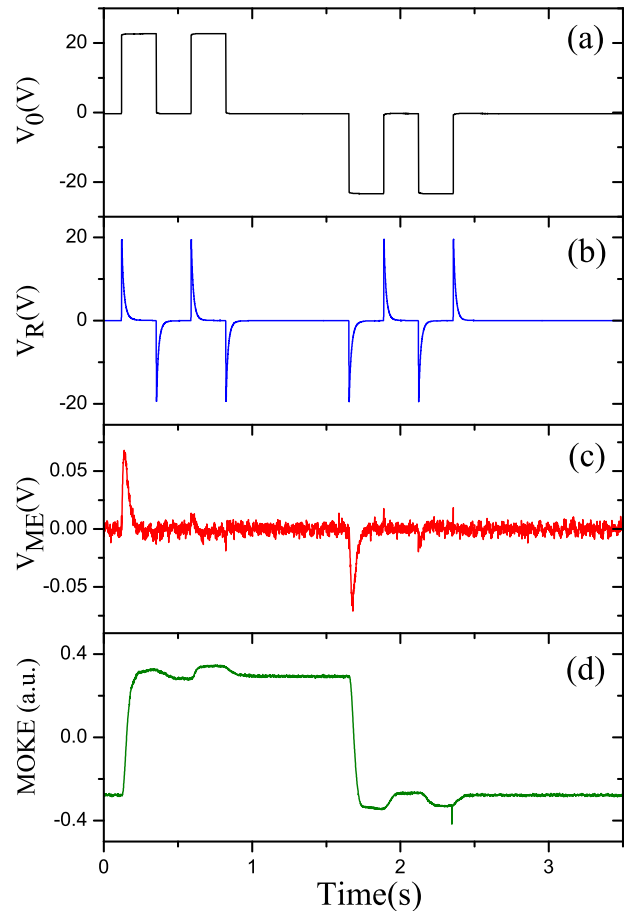


FIG. 2. (a) Sequence of the electrical pulses applied to the MELRAM cell; (b) V_R voltage detected on the resistance connected in series; (c) Magneto-electric voltage obtained by subtraction $V_{ME} = V_R(H) - V_R(0)$; and (d) Variation of magnetization projection on the easy axis detected by the magneto-optic Kerr effect.

magnetization according to the pulse polarity. The application of the “reading” electric pulse with the same polarity does not change the magnetic state and no ME response is detected. However, if the “reading” pulse polarity is changed, a magnetization switch is induced and the ME response is observed. Figure 2(d) shows the corresponding behavior of the magnetization projection on the easy axis of the cell. The last measurements were made using the magneto-optic Kerr effect.

The maximum value of the observed ME signal is equal to $V_{ME} = 75$ mV. The theoretical value predicted by Eq. (14) can be estimated using the thickness of the magnetic layer $h^m = 200$ nm, magnetoelastic constant $B = -7$ MPa,³³ and the following parameters of PMN-PT:³⁴ $d_{31} = 610$ C/N, $d_{32} = -1883$ C/N, $\epsilon_{33} = 4033$. The estimated signal $V_{ME} = 98$ mV is close to the experimental value.

The obtained theoretical and experimental results show the feasibility of the two basic operations of recording and reading of information stored in the magnetic subsystem using electric field pulses applied to the MELRAM cell. The main challenge for the implementation of the ME readout lies in the separation of the magneto-electrically induced potential V_{ME} from the V_0 applied voltage for the magnetic state identification. Here, the V_{ME} signal was extracted by a mathematical subtraction of the experimental data. In a real cell, the separation can be achieved by using a Wheatstone bridge scheme with a passive nonmagnetic capacitor in the branch parallel to the cell. Moreover, the experiment under consideration was performed on a cell of a millimetric size. Nevertheless, according to Eq. (8), the ME potential does not depend on the thickness of the piezoelectric layer when $h^p \gg h^m$ nor on the in-plane cell dimensions (except for the lateral effects from the fringing field³⁵). It means that the ME readout principle allows for the cell down-scaling without any visible decrease of the ME signals. A drawback of this energy efficient readout approach is that it is a destructive one when the readout voltage pulse switches the magnetization. Nevertheless, by using the output electric signal generated by the switch to trigger a delayed writing pulse with an opposite polarity, the initial state of the magnetic system can be restored automatically.

The authors thank A. Vlasyuk for his participation in the experimental measurements. This work was supported by the RFBR 16-29-14022 Grant, the StartAirr program MELRAM of the Hauts-de-France, as well as the RENATECH technological network.

¹ITRS, <http://www.itrs.net/Links/2013ITRS/2013Chapters/2013ERD.pdf> for “Emerging research devices,” Technical Report, The International Technology Roadmap for Semiconductors, 2013.

²A. Chen, “Extended papers selected from ESSDERC 2015,” *Solid-State Electron.* **125**, 25 (2016).

³M. Kryder and C. Kim, *IEEE Trans. Magn.* **45**, 3406 (2009).

⁴J. Akerman, *Science* **308**, 508 (2005).

⁵A. D. Kent and D. C. Worledge, *Nat. Nanotechnol.* **10**, 187 (2015).

⁶M. Cubukcu, O. Boulle, M. Drouard, K. Garello, C. O. Avci, I. M. Miron, J. Langer, B. Ocker, P. Gambardella, and G. Gaudin, *Appl. Phys. Lett.* **104**, 042406 (2014).

⁷M. Fiebig, *J. Phys. D.: Appl. Phys.* **38**, R123 (2005).

⁸N. A. Spaldin and M. Fiebig, *Science* **309**, 391 (2005).

⁹X. He, Y. Wang, N. Wu, A. N. Caruso, E. Vescovo, K. D. Belashchenko, P. A. Dowben, and C. Binek, *Nat. Mater.* **9**, 579 (2010).

¹⁰J. G. Alzate, P. K. Amiri, P. Upadhyaya, S. S. Cherepov, J. Zhu, M. Lewis, R. Dorrance, J. A. Katine, J. Langer, K. Galatsis, D. Markovic, I. Krivorotov, and K. L. Wang, in 2012 International Electron Devices Meeting, 10–13 December 2012, pp. 29.5.1–29.5.4.

¹¹S. Fusil, V. Garcia, A. Barthelemy, and M. Bibes, *Annu. Rev. Mater. Res.* **44**, 91 (2014).

¹²F. Matsukura, Y. Tokura, and H. Ohno, *Nat. Nanotechnol.* **10**, 209 (2015).

¹³J. v d. Boomgaard, A. M. J. G. van Run, and J. Van Suchtelen, “Ferroelectrics,” *Ferroelectrics* **14**, 727 (1976).

¹⁴N. Tiercelin, Y. Dusch, V. Preobrazhensky, and P. Pernod, *J. Appl. Phys.* **109**, 07D726 (2011).

¹⁵N. Tiercelin, Y. Dusch, A. Klimov, S. Giordano, V. Preobrazhensky, and P. Pernod, *Appl. Phys. Lett.* **99**, 192507 (2011).

¹⁶J.-M. Hu, Z. Li, L.-Q. Chen, and C.-W. Nan, *Nat. Commun.* **2**, 553 (2011).

¹⁷T. Wu, A. Bur, K. Wong, P. Zhao, C. S. Lynch, P. K. Amiri, K. L. Wang, and G. P. Carman, *Appl. Phys. Lett.* **98**, 262504 (2011).

¹⁸M. Ghidini, R. Pellicelli, J. Prieto, X. Moya, J. Soussi, J. Briscoe, S. Dunn, and N. Mathur, *Nat. Commun.* **4**, 1453 (2013).

¹⁹A. K. Biswas, S. Bandyopadhyay, and J. Atulasimha, *Appl. Phys. Lett.* **105**, 072408 (2014).

²⁰S. Giordano, Y. Dusch, N. Tiercelin, P. Pernod, and V. Preobrazhensky, *Phys. Rev. B* **85**, 155321 (2012).

²¹S. Giordano, Y. Dusch, N. Tiercelin, P. Pernod, and V. Preobrazhensky, *J. Phys. D.: Appl. Phys.* **46**, 325002 (2013).

²²A. K. Biswas, S. Bandyopadhyay, and J. Atulasimha, *Appl. Phys. Lett.* **104**, 232403 (2014).

²³N. Tiercelin, Y. Dusch, S. Giordano, A. Klimov, V. Preobrazhensky, and P. Pernod, “Strain Mediated Magnetoelectric Memory,” in *Nanomagnetic and Spintronic Devices for Energy Efficient Computing* (Wiley and Sons., 2015), Chap. 8.

²⁴J. L. Hockel, S. D. Pollard, K. P. Wetzlar, T. Wu, Y. Zhu, and G. P. Carman, *Appl. Phys. Lett.* **102**, 242901 (2013).

²⁵Y. Dusch, N. Tiercelin, A. Klimov, S. Giordano, V. Preobrazhensky, and P. Pernod, *J. Appl. Phys.* **113**, 17C719 (2013).

²⁶J. Cui, C.-Y. Liang, E. A. Paisley, A. Sepulveda, J. F. Ihlefeld, G. P. Carman, and C. S. Lynch, *Appl. Phys. Lett.* **107**, 092903 (2015).

²⁷Z. Zhao, M. Jamali, N. D’Souza, D. Zhang, S. Bandyopadhyay, J. Atulasimha, and J.-P. Wang, *Appl. Phys. Lett.* **109**, 092403 (2016).

²⁸Y. Dusch, V. Rudenko, N. Tiercelin, S. Giordano, V. Preobrazhensky, and P. Pernod, *Nanomater. Nanostruct.* **2**, 44 (2012), see <http://www.radiotec.ru/catalog.php?cat=jr18&art=11419>.

²⁹A. Jaiswal and K. Roy, *Sci. Rep.* **7**, 39793 (2017).

³⁰J. Z. Sun, *Proc. SPIE* **9931**, 993113 (2016).

³¹W. Zhao, T. Devolder, Y. Lakys, J. Klein, C. Chappert, and P. Mazoyer, in *Proceedings of the 22th European Symposium on the Reliability of Electron Devices, Failure Physics and Analysis*, [*Microelectron. Rel.* **51**, 1454 (2011)].

³²N. Tiercelin, Y. Dusch, V. Preobrazhensky, and P. Pernod, “Magnetoelectric memory,” Granted Patents FR2961632B1, US8908422B2, RU2573207C2, and JP5784114B2.

³³N. Tiercelin, V. Preobrazhensky, P. Pernod, and A. Ostaschenko, *Appl. Phys. Lett.* **92**, 062904 (2008).

³⁴F. Wang, L. Luo, D. Zhou, X. Zhao, and H. Luo, *Appl. Phys. Lett.* **90**, 212903 (2007).

³⁵J. Scott, *Ferroelectric Memories* (Springer-Verlag, Berlin, Heidelberg, 2000).